Optik 164 (2018) 424–432

Contents lists available at ScienceDirect

Optik

journal homepage: www.elsevier.de/ijleo

Original research article

XRD, SEM, XPS studies of Sb doped ZnO films and electrical properties of its based Schottky diodes

Yasemin Caglar, Mujdat Caglar*, Saliha Ilican

Anadolu University, Science Faculty, Physics Department, Eskisehir, Turkey

ARTICLE INFO

Article history:
Received 27 November 2017
Received in revised form 5 March 2018
Accepted 6 March 2018

Keywords:
Sb doped ZnO
XPS
Schottky diode
Cheung function

ABSTRACT

This work presents both the morphological and structural characterizations of ZnO depending on the Sb doping and the electrical characterization of ZnO based Schottky diodes grown on ITO substrates by sol gel dip coating method. In Schottky diode fabrication, undoped and Sb doped ZnO were used, which exhibit n-type and p-type behavior, respectively. For undoped and Sb doped ZnO, Pt and Al were used as a metal contact. For the surface morphology, scanning electron microscopy (SEM) has been carried out and the surface properties that play an important role on the Schottky diode performance were characterized by SEM. X-ray diffraction (XRD) measurements revealed that crystal quality got worse and crystallite size decreased with Sb incorporation. The presence of Sb in the ZnO was confirmed by X-ray photoelectron spectroscopy (XPS). Undoped and Sb doped ZnO based Schottky diodes were fabricated and their electrical properties were carried out in dark. The diode parameters such as ideality factor (n), barrier height (φ_B) and series resistance (R_s) were systematically analyzed by using thermionic emission theory and Cheung's method.

1. Introduction

Zinc oxide (ZnO) films have been studied with many researches due to intrinsic properties such as wide band gap (3.2 eV), large exciton binding energy (60 meV), low production cost and bio-safety. This material have attracted attention in scientific and technological communities because of their application in several devices as field effect transistors [1–3], heterojunction and Schottky diodes [4–6], sensors [7,8] and solar cells [9,10]. Among these devices, metal-semiconductor Schottky barrier diodes based on ZnO films are basic building blocks of electronic device.

The ZnO-based Schottky diode was investigated in 2002 [11] in first time. The authors reported that silver Schottky contacts were fabricated on n-ZnO epilayers, which were grown on R-plane sapphire substrates by metalorganic chemical-vapor deposition. The flat band barrier height was determined to be 0.89 and 0.92 eV by current-voltage and capacitance-voltage measurements, respectively. The ideality factor was found to be 1.33. There are a number of works with metal/ZnO Schottky diodes in available literature. Most of these diodes were used n-type ZnO. However, the p-type doping of ZnO is still a challenge, which becomes the main hindrance in the development of ZnO-based optoelectronic devices [12].

The doped of ZnO with group I (Li, Na, K) or group V (N, As, Sb) elements will change the conductivity of type. Theoretically, group-I elements as p-type dopants in ZnO are far better than group-V elements. Bagheri et al. [13] deposited Li doped ZnO by sol gel. Authors reported that the conductivity of the ZnO film doped with optimized Li ratio (15 at%) changed from

* Corresponding author.
E-mail address: mcaglar@anadolu.edu.tr (M. Caglar).

https://doi.org/10.1016/j.ijleo.2018.03.017
0030-4026/

n-type to p-type. Chelouche et al. [14] prepared Na doped ZnO thin films onto quartz substrate by sol gel deposition. They reported that p-type conductivity was observed only on the 3 at % Na-doped sample and with an increasing Na concentration it was observed a decrease in the average grain size and surface roughness. Tay et al. [15] deposited K defect in ZnO films grown using the aqueous solution route, which explains the switching between p- and n-type conductivities under different doping or thermal annealing conditions. They emphasized that the success of p-type doping depends on the aqueous growth conditions and the concentration ratio of K^+ /Zn^{2+} and solution pH are important parameters in this success.

Sb doped ZnO films have been deposited by metal-organic chemical vapour deposition (MOCVD) [8], spray pyrolysis [9,10], rf sputtering [11], sol gel spin coating [12,13]. Among many techniques for preparing Sb doped ZnO films, sol gel dip coating has many advantages such as simple, inexpensive, and having large area applications.

To the best of our knowledge, there is only one study on the fabrication and characterization of Sb doped ZnO based Schottky diode in the available literature. In this work, Mandalapu et al. [16,17] investigated the electrical properties of Sb doped ZnO films grown on n-Si by molecular beam epitaxy using Al/Ti metal. In their investigations they used the current-voltage (*I-V)* and capacitance-voltage (*C-V)* characterizations. Used Al/Ti contacts exhibited Schottky diode behavior with a barrier height of 0.8 eV estimated from the *C-V* measurements. It was also reported that the ideality factor or precise barrier height was not determined because of not being known the actual area of device.

Although many researchers have studied the preparation and characterization of Sb doped ZnO, as mentioned above there is only one report about their Schottky diodes applications. Of course, a reason of this can be the challenge of obtaining successfully p-type ZnO and its fabrication as an Schottky diode. In the work of Mandalapu et al. [17], both Schottky and ohmic contacts were taken from the top and as a result, the detailed investigations of diode parameters were not made due to the unknown of actual area of the device. But, in our work, ITO substrate was used and there was no such problem. Therefore, the importance of this study is to contribute to the literature in this subject, where there is little work and to consist of detailed and systematic characterizations presenting the effect of Sb incorporation. In this paper, it has been investigated how Sb incorporation influences the structural, morphological and electrical properties of the ZnO films which are grown on ITO by a sol gel dip coating technique. And also, it has been carried out the electrical characterization of *Pt/n-ZnO/ITO, Al/p-ZnO:0.2%Sb/ITO and Al/p-ZnO:0.4%Sb/ITO* Schottky diodes by using measurements.

2. Experimental

The undoped and Sb doped ZnO films were deposited by sol gel dip coating method onto ITO substrates. Zinc acetate dihydrate [$Zn(CH_3COO)_2{\cdot}2H_2O$] (ZnAc) and antimony chloride [$SbCl_3$] (SbCl) were used as a starting material and dopant source. 2-Methoxyethanol [$C_3H_8O_2$] and ethanolamine [C_2H_7NO] (MEA) as a solvent and stabilizer, respectively. The molar ratio of MEA to ZnAc was maintained at 1:1 and the concentration of ZnAc and SbCl was 0.35 M. These solutions were mixed together in different volume proportions 0.2 and 0.4%. In order to yield a clear, homogeneous and transparent solution, it was stirred for 2 hours at 60 °C using a magnetic stirrer. After stirring process, the solution was infiltrated using filter paper. The ITO substrates were cleaned in methanol, acetone using an ultrasonic cleaner. The cleaned ITO substrate was placed on the sample holder and was dipped at withdrawn speed of 8 mm/min. The dip coated films were preheated at 300 °C for 10 min in a furnace. This coating/drying procedure was repeated ten times, before the films were annealed at 600 °C in air for 60 min. Then, Schottky contacts were made onto surface of the film, patterned with a shadow mask by circular dots of 0.5 mm in diameter. Evaporation and sputtering methods were used to be formed aluminum and platinum contacts on the surface, respectively. The fabricated *Pt/n-ZnO/ITO, Al/p-ZnO:0.2%Sb/ITO and Al/p-ZnO:0.4%Sb/ITO* Schottky diodes are named SD0, SD2 and SD4 respectively. The schematic structure of these Schottky diodes is illustrated in Fig. 1.

X-ray diffraction patterns (XRD) were obtained with a BRUKER D2 Phaser Series X-ray automatic diffractometer using the $Cu_{K\alpha}$ radiations (λ = 1.54059 Å) in the 2θ range between 30° and 60° at room temperature with a scanning step size of 0.02°. The diffractometer reflection was taken at room temperature. Surface morphology was studied using ZEISS Ultraplus model field emission scanning electron microscopy (SEM). VAKSIS PVD-HANDY/MT/101T thermal evaporation and VAKSIS Midas PVD-MT/1M3T, Turkey sputter systems were used for the evaporation of Al and sputtering of Pt contacts, respectively. The

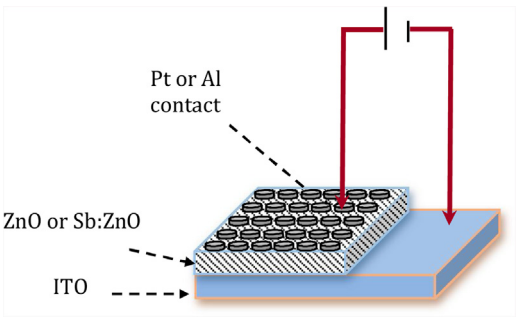

Fig. 1. The schematic diagram of the fabricated Schottky diodes.

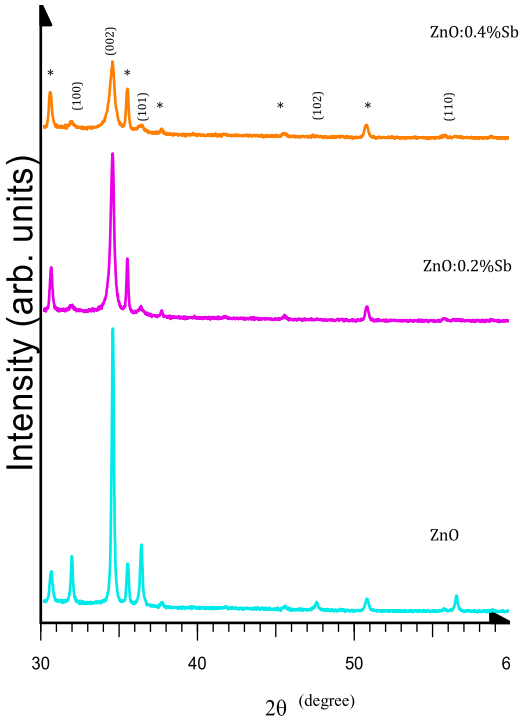

Fig. 2. XRD patterns of the undoped and Sb-doped ZnO films (*: Si substrate).

Table 1
Structural parameters of the undoped and Sb-doped ZnO films.

Sample name	(hkl)	2θ (degree)	d (Å)	FWHM (degree)	D (nm)
ZnO	(100)	31.835	2.8070	–	–
	(002)	34.478	2.5976	0.168	48
	(101)	36.317	2.4702	–	–
ZnO:0.2%Sb	(100)	31.813	2.8107	–	–
	(002)	34.447	2.6014	0.260	33
	(101)	36.281	2.4741	–	–
ZnO:0.4%Sb	(100)	31.815	2.8114	–	–
	(002)	34.435	2.6024	0.347	25
	(101)	36.272	2.4746	–	–

electrical measurements were performed at room temperature in the Van der Pauw configuration by ECOPIA HMS-5000 Hall measurement system. X-ray photoelectron spectroscopy (XPS, SPECS GmbH, Germany) was used to identify the presence of Sb in the ZnO and bonding states of related elements using $Al_{K\alpha}$ X-rays. The *I-V* characterizations were carried out by using a KEITHLEY 4200 SCS and SIGNATONE probe station inside dark box.

3. Results and discussion

3.1. XRD studies of undoped and Sb doped ZnO films

The crystal quality and orientation of the Sb doped ZnO films were considered by XRD patterns. Fig. 2 shows the XRD spectra all of the films. The presence of several peaks in the XRD reveals that the films are polycrystalline nature with a hexagonal wurtzite structure (JCPDS card file no: 361451). Five main peaks are observed in all the films and the most intense peak belongs to the (002) plane. As shown in Fig. 2, the crystal quality of the films decreased with the addition of Sb and it causes a decrease in intensity of the peaks. The *2θ, d, FWHM* values of the undoped and Sb doped films were given in Table 1. From this Table, the (002) peak positions of the films shifted toward a lower diffracting angle with increasing Sb doping. Although, no diffraction peaks of Sb or SbO are observed in the XRD patterns, but the presence of Sb_2O_3 phase was confirmed by XPS, the reason of this shifting can be attributed to the fact that the Sb^{+3} ionic radius of 0.78 nm in the ZnO lattice is larger than the Zn^{+2} ionic radius of 0.074 nm, which causes the increase of the inter planar spacing (*d*) [18,19]. These changes in both inter planar spacing and diffracting angle explain the substitution of Sb^{+3} into the Zn site of the host

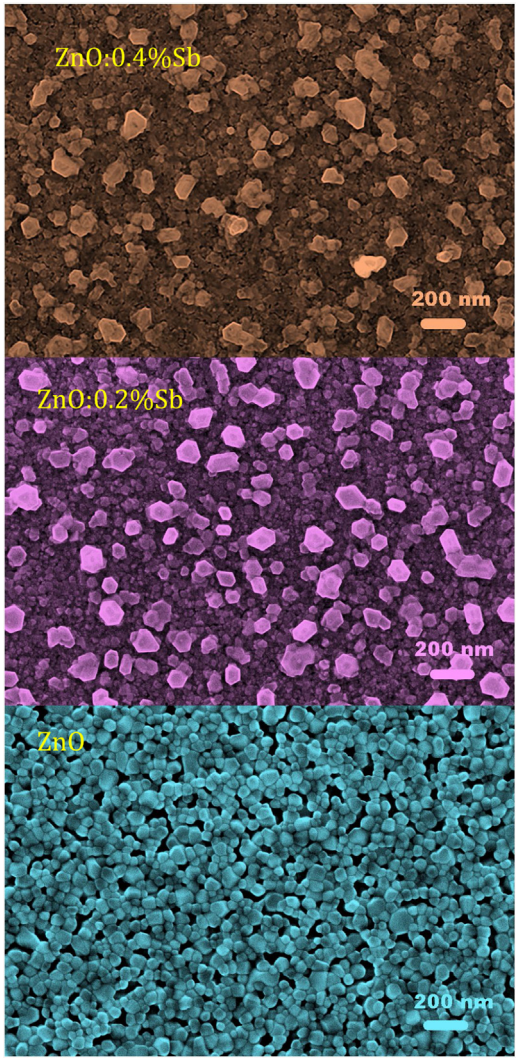

Fig. 3. Top view SEM images of the undoped and Sb-doped ZnO films.

ZnO [20,21]. The crystallite size (D) of undoped and Sb doped ZnO films was determined using the Scherrer's formula [22] and given in Table 1. From this Table, the crystallite size is decreased with Sb doping. Similar results have been reported by Omidi et al. [23] and Ravichandran et al. [24]. This decrease in crystallite size confirms the deterioration in the crystal quality of the films.

3.2. SEM studies of undoped and Sb doped ZnO films

SEM has been used to analyze the surface of the coated films on ITO. Fig. 3 illustrates the surface images of both undoped and Sb doped ZnO films. In the ZnO image, grain boundaries and particles distributed almost homogeneously have been clearly seen and almost smooth surface has been also seen although there are slight voids between the particles. After the incorporation of small amount of Sb, the particles having generally hexagonal structure, changing sizes about between 50 nm and 150 nm and randomly distributed are shown on the surface. As seen in this image, it causes to form almost roughly surface. But at the same time, the small particles that are decreased by Sb doping are shown at the background. This decrease in the particle size with Sb doping is also observed in the XRD results. With a little more incorporation of Sb, the grain boundaries at the background disappears, hexagonal shapes of the particles that randomly distributed on the surface disappear and their numbers decrease as seen in the first SEM image. Of course, ZnO:0.4%Sb film has also almost roughly surface like the other doped film and this surface property plays a crucial role on the electrical properties of Schottky diode.

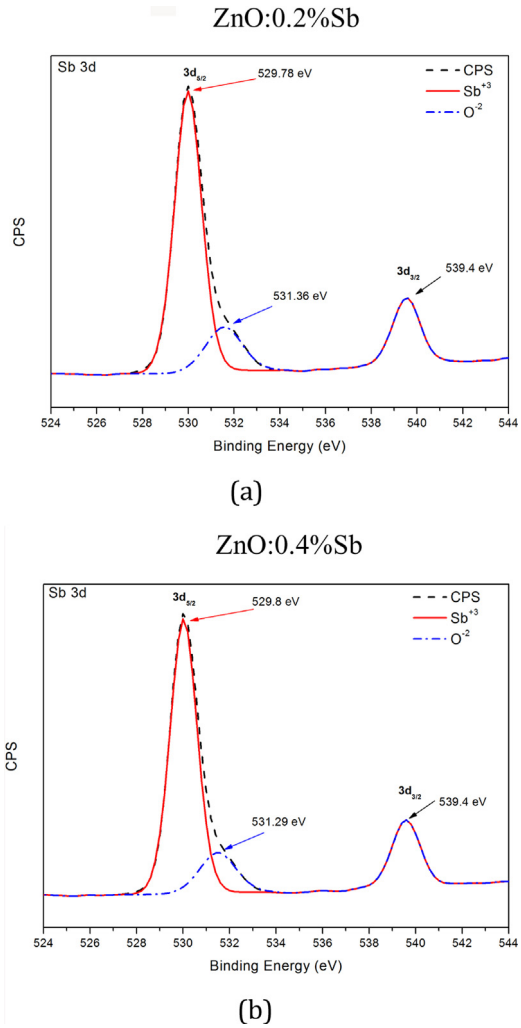

Fig. 4. The peaks corresponding to the Sb3d orbital for the Sb doped ZnO films.

3.3. XPS studies of undoped and Sb doped ZnO films

X-ray photoelectron spectroscopy (XPS), which is one of the most substantial material characterization techniques, was used to characterize the surface of both undoped and Sb doped ZnO films grown by sol gel dip coating on the ITO and the bonding states of related elements on the surface using $Al_{K\alpha}$ X-rays. In this analysis, the C1s peak at 284.6 eV was used for the calibration without any etching process being applied. The measured chemical states related to Sb 3d confirm that Sb element was successfully incorporated into ZnO lattice as a dopant and the observed Sb $3d_{3/2}$ peaks at 539.4 eV in Fig. 4(a) and (b) are evidence of this. The peaks at 531.36 eV and 531.29 eV that observed in Fig. 4 are attributed to O 1s mainly corresponding to the O^{2-} in ZnO [25,26] and the superimposition of Sb $3d_{5/2}$ and O1s makes it difficult to determine the exact amount of Sb content in ZnO. Therefore, the presence of Sb in the ZnO is confirmed but its exact ration is not determined. Binding energies of 529.78 eV and 529.8 eV for Sb $3d_{5/2}$ and 539.4 eV for Sb $3d_{3/2}$ are characteristic of the Sb^{+3} in Sb_2O_3 while Sb_2O_3 phase is not observed in the XRD patterns. Furthermore, the p-type conductivity behavior observed from the Hall effect measurements also confirms the substitution of Sb^{+3} on Zn^{+2} site. As the proposed by Senthil et al [27] and the mentioned in previous works [28–30], when Sb is in 3+ state, which means that the defect complex acts as an acceptor, it is expected that Sb doped ZnO behaves as a p-type material.

3.4. Electrical transport characterization of undoped and Sb doped ZnO films

Hall measurements were used to identify p-type behavior of ZnO with Sb incorporation. As a results of these measurements, the resistivity (ρ), carrier concentration (n) and mobility (μ) values of the undoped and Sb doped ZnO films were determined and Van der Pauw configuration was used in these measurements. These electrical parameters and their con-

Table 2
The electrical transport values of the films.

Sample name	Conduction type	ρ (ohm cm)	μ ($cm^2 V^{-1} s^{-1}$)	Carrier concentration $X10^{15}$ (cm^{-3})
ZnO	n	62.1	0.29	8.15
ZnO:0.2%Sb	p	239	3.42	3.08
ZnO:0.4%Sb	p	394	3.50	4.86

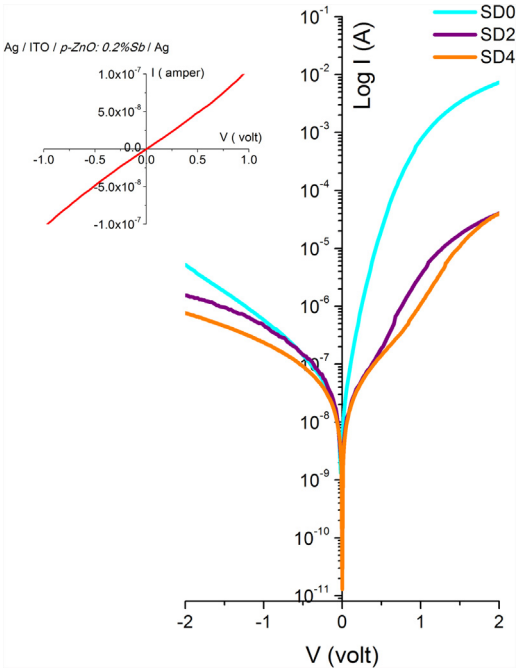

Fig. 5. Semilog *I-V* characteristics of the fabricated schottky diodes.

ductivity types of undoped and doped are given in Table 2. While the undoped ZnO exhibits n-type conductivity behavior, Sb doped ZnO exhibits p-type. Therefore, it is understood that a small amount of Sb is sufficient to change the conductivity type. As seen in Table 2, as Sb doping increases, the mobility and carrier concentration increase and depending on this, the resistivity decreases. Therefore, the incorporation of Sb into the ZnO both changes conductivity type and causes a slight improvement in conductivity.

3.5. *I-V characteristics of Pt/n-ZnO/ITO and Al/p-ZnO:Sb/ITO Schottky diodes*

Room temperature current-voltage (*I-V)* characteristics of *Pt/n-ZnO/ITO and Al/p-ZnO:Sb/ITO* Schottky diodes formed by selecting of appropriate metals depending on the work function values are shown in Fig. 5. In this figure, it can be seen that the obtained metal-semiconductor contacts have a rectifying behavior and this behavior is getting worse with Sb doping. The rectification ratio that is about 10^3 at first decreases drastically with incorporation of Sb into the ZnO. In this structure, in order to determine that there is no contribution from p-ZnO:Sb/ITO interface to the rectifying, the ohmic behavior of this contact was checked from the I-V graph of p-ZnO:Sb/ITO structure obtained by applying silver paste both on ITO and film surface and it is given in Fig. 5.

The observed non-linear behavior can be described with the thermionic emission model by the following relation [31]

$$I = I_o \left[\left(\exp\left(\frac{qV}{nkT}\right) - 1 \right] \right. \tag{1}$$

where I_o, q, n, k, T, V are the saturation current, the electronic charge, the diode ideality factor, the Boltzmann constant and the temperature (in Kelvin) and the applied voltage, respectively. In such a Schottky contact, n values which is one of the important parameters that show the quality of a metal-semiconductor contact are calculated by the slope of the linear regions for low voltage biases of *I-V* curves. Pre-exponential factor I_0 in Eq. (1) is given by

$$I = AA^*T^2 exp\left(-\frac{q\Phi_b}{kT}\right) \tag{2}$$

Table 3
The diode parameters of the fabricated Schottky diodes.

Diode	I-V		Cheung-Cheung		
			Cheung	H function	
	n	Φ_b (eV)	n	R_s (kΩ)	Φ_b (eV)
SD0	3.01	0.66	7.49	0.12	0.41
SD2	6.45	0.70	7.94	21.57	0.42
SD4	10.98	0.68	8.54	14.66	0.41

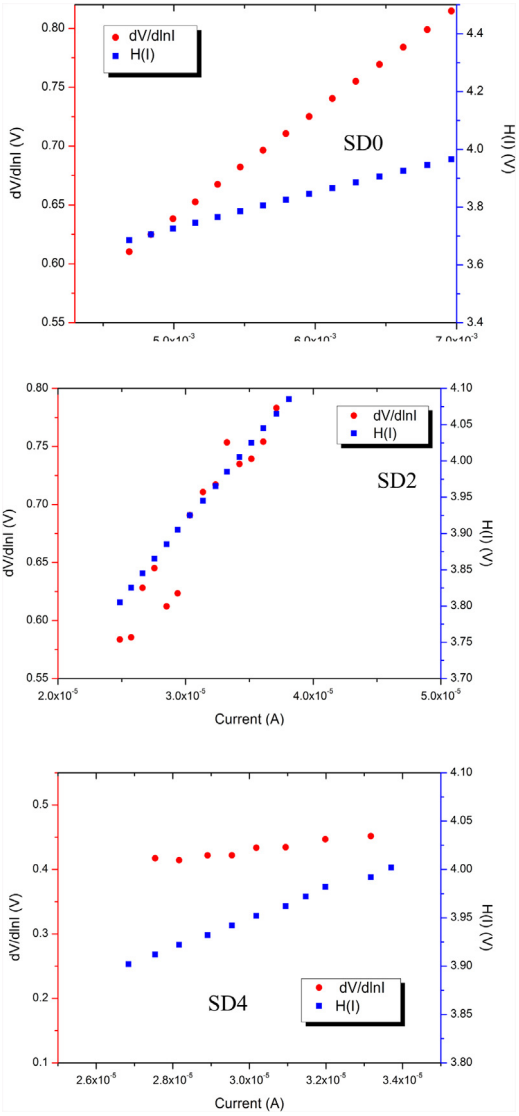

Fig. 6. The forward bias *dV/d(lnI)-I* and *H(I)-I* plots of the fabricated schottky diodes.

where A is the diode contact area (approximately 0.2×10^{-2} cm^2), A^* is the Richardson constant for ZnO ($A^* = 32$A/cm^{2}K^2) and is $\Phi_b$the Schottky barrier height which is the second important parameter that presents the quality of contact and it can be estimated by Eq. (2). The n and Φ_b values gotten from *I-V* plot are tabulated in Table 3. The expected value of n for ideal Schottky contact should be unity. But the n values that larger than 1 exhibit the deviations from the ideal contact and how the incorporation of Sb into the ZnO strongly affects the diode performance. Of course, not only the getting worse of the surface conditions depending on the Sb incorporation but also the getting worse the crystal quality play a crucial role on the quality of metal-semiconductor interface. Both XRD spectra and SEM images support these results. Therefore, the presence of inhomogeneity in barrier height and presence of interface states can be attributed to the reason of being larger

than unity of ideality factor with no significant change in the barrier height. In a study reported by Mosbacker et al. [32], it was concluded that the deep level defects could have a major impact on Schottky barrier, and they reported 0.43 eV and 3.57 for Schottky barrier and ideality factor in Pt/ZnO Schottky barrier which has high defect level. These values worse than ours exhibit that our ZnO structure can have high defect level.

Serial resistance (R_s), which is both the third important parameters of metal-semiconductor contact and one of the greatest reasons of the deviation of ideal diode behavior, can affect the electrical performance of Schottky diode and can be evaluated by using Cheung's method in the high current region where *I-V* characteristic deviates from the linearity. In this method, which can be also determined n and φ_B values, the forward bias *I-V* characteristics of a device having series resistance is given as

$$I = I_o \exp\left(\frac{q(V - IR_s)}{nkT}\right) \tag{3}$$

The following equations is used to determine the n, R_s and φ_B values,

$$\frac{dV}{d(\ln I)} = IR_s + \frac{nkT}{q} \tag{4}$$

$$H(I) = n\phi_B + IR_s \tag{5}$$

$$H(I) = V - \frac{nkT}{q}\ln\left(\frac{I}{AA^*T^2}\right) \tag{6}$$

The forward bias *dV/d(lnI)-I* plots of the Schottky diodes are given in Fig. 6. The intercept gives the n value of these diodes. These calculated values for n is tabulated in Table 3. In these observed differences between the n values that were obtained from the forward bias semilog *I–V* plots and from the *dV/d(InI)-I* plots, undesirable interface states and different voltage ranges which are used in the calculations can play an important role [33].

The plots of *H(I)* versus *I* are shown in Fig. 6 and the slope of this plot gives R_s value and intercept gives the φ_B value. The calculated values are given in Table 2. R_s values calculated from both *dV/d(InI)-I* plots and *H(I)* function are close to each other and increase with Sb doping. This increase in the R_s with increase in n is expected result because one of the reasons of deviation from the ideality is R_s as mentioned before. And also, the calculated R_s values are in good agreement with previous reported works [kaynak]. As seen in Table 2, Φ_b values are almost same but smaller than that of the calculated from the forward bias semilog *I-V* plots. The reason of this difference may be due to the different voltage ranges in which both methods are applied.

4. Conclusion

In this study, sol gel dip coating method was used to deposit undoped and Sb doped ZnO films on the ITO substrate. To get p-type ZnO, the small amounts of Sb ratio of 0.2 and 0.4 were used. As hall measurements confirm the p-type conductivity, XPS results also confirm the presence and ionic state of Sb. Sb incorporation caused the occurrence of p-type behavior, but at the same time, it leads to deterioration of crystal structure. It also adversely affected the surface properties, which plays an important role on the electrical performance of the Schottky diode. The all Schottky diodes fabricated using both n-type undoped ZnO and Sb doped ZnO which was successfully formed as a p-type exhibited a rectifying behavior. The diode parameters such as n, φ_B and R_s were calculated by using thermionic emission theory and Cheung's method and in these parameters, the effect of Sb incorporation was reported. The obtained results revealed that p-type ZnO can be successfully produced and these Schottky diodes can be easily used in the optoelectronic applications provided that the surface properties are improved.

Acknowledgement

This work was supported by Anadolu University Commission of Scientific Research Projects under Grant Nos. 1305F082 and 1402F055. The authors would like to thank Dr. Mustafa KULAKCI for his help in sputtering Pt contacts.

References

[1] C. Florica, A. Costas, A. Kuncser, N. Preda, I. Enculescu, High performance FETs based on ZnO nanowires synthesized by low cost methods, Nanotechnology 27 (475303) (2016), http://dx.doi.org/10.1088/0957-4484/27/47/475303.
[2] S. Aksoy, S. Ruzgar, Effect of N doped on optical properties of ZnO film deposited by sol gel, J. Mater. Elec. Devices 1 (2016) 1–4.
[3] Y. Caglar, M. Caglar, S. Ilican, S. Aksoy, F. Yakuphanoglu, Effect of channel thickness on the field effect mobility of ZnO-TFT fabricated by sol gel process, J. Alloys Compd. 621 (2015) 189–193, http://dx.doi.org/10.1016/j.jallcom.2014.09.190.
[4] I. Orak, A. Kocyigit, A. Turut, The surface morphology properties and respond illumination impact of ZnO/n-Si photodiode by prepared atomic layer deposition technique, J. Alloys Compd. 691 (2017) 873–879, http://dx.doi.org/10.1016/j.jallcom.2016.08.295.
[5] A.B. Yadav, S. Jit, Particle size effects on the hydrogen sensing properties of Pd/ZnO Schottky contacts fabricated by sol–gel method, Int. J. Hydrogen Energy 42 (2016) 1–9, http://dx.doi.org/10.1016/j.ijhydene.2016.08.201.
[6] J. Kim, K.H. Baik, S. Jang, Schottky contact on hydrothermally grown a-plane ZnO for hydrogen sensing and UV detection, Curr. Appl. Phys. 16 (2016) 221–225, http://dx.doi.org/10.1016/j.cap.2015.11.014.

[7] Y. Zhou, X. Lin, Y. Wang, G. Liu, X. Zhu, Y. Huang, et al., Study on gas sensing of reduced graphene oxide/ZnO thin film at room temperature, Sens. Actuators B: Chem. 240 (2017) 870–880, http://dx.doi.org/10.1016/j.snb.2016.09.064.
[8] S. Devendiran, D. Sastikumar, Gas sensing based on detection of light radiation from a region of modified cladding (nanocrystalline ZnO) of an optical fiber, Opt. Laser Technol. 89 (2017) 186–191, http://dx.doi.org/10.1016/j.optlastec.2016.10.013.
[9] M. Hala, H. Kato, M. Algasinger, Y. Inoue, G. Rey, F. Werner, et al., Improved environmental stability of highly conductive nominally undoped ZnO layers suitable for n-type windows in thin film solar cells, Sol. Energy Mater. Sol. Cells 161 (2017) 232–239, http://dx.doi.org/10.1016/j.solmat.2016.11.015.
[10] J. Duan, Q. Xiong, H. Wang, J. Zhang, J. Hu, ZnO nanostructures for efficient perovskite solar cells, J. Mater. Sci.: Mater. Electron. 28 (2017) 60–66, http://dx.doi.org/10.1007/s10854-016-5492-3.
[11] H. Sheng, S. Muthukumar, N.W. Emanetoglu, Y. Lu, Schottky diode with Ag on (1120) epitaxial ZnO film, Appl. Phys. Lett. 80 (2002) 2132–2134, http://dx.doi.org/10.1063/1.1463700.
[12] L.P. Dai, H. Deng, F.Y. Mao, J.D. Zang, The recent advances of research on p-type ZnO thin film, J. Mater. Sci.: Mater. Electron. 19 (2008) 727–734, http://dx.doi.org/10.1007/s10854-007-9398-y.
[13] N. Bagheri, M.H.M. Ara, N. Ghazyani, Characterization and doping effects study of high hole concentration Li-doped ZnO thin film prepared by sol gel method, J. Mater. Sci.: Mater. Electron. 27 (2016) 1293–1298, http://dx.doi.org/10.1007/s10854-015-3888-0.
[14] A. Chelouche, T. Touam, F. Boudjouan, D. Djouadi, R. Mahiou, A. Bouloufa, et al., Na doping effects on the structural, conduction type and optical properties of sol gel ZnO thin films, J. Mater. Sci.: Mater. Electron. 28 (2017) 1546–1554, http://dx.doi.org/10.1007/s10854-016-5694-8.
[15] C.B. Tay, J. Tang, X.S. Nguyen, X.H. Huang, J.W. Chai, V.T. Venkatesan, et al., Low temperature aqueous solution route to reliable p-type doping in ZnO with K: growth chemistry, doping mechanism, and thermal stability, J. Phys. Chem. C 116 (2012) 24239–24247, http://dx.doi.org/10.1021/jp3070757.
[16] L.J. Mandalapu, F.X. Xiu, Z. Yang, D.T. Zhao, J.L. Liu, P-type behavior from Sb-doped ZnO heterojunction photodiodes, Appl. Phys. Lett. 88 (2006), http://dx.doi.org/10.1063/1.2186516.
[17] L.J. Mandalapu, F.X. Xiu, Z. Yang, J.L. Liu, Al/Ti contacts to Sb-doped p -type ZnO, J. Appl. Phys. 102 (2007), http://dx.doi.org/10.1063/1.2759874.
[18] Y. Yang, J. Qi, Q. Liao, Y. Zhang, L. Tang, Z. Qin, Synthesis and characterization of Sb-doped ZnO nanobelts with single-side zigzag boundaries, J. Phys. Chem. C 112 (2008) 17916–17919, http://dx.doi.org/10.1021/jp8064213.
[19] S. Ilican, Y. Caglar, M. Caglar, F. Yakuphanoglu, J. Cui, Preparation of Sb-doped ZnO nanostructures and studies on some of their properties, Phys. E: Low-Dimens. Syst. Nanostruct. 41 (2008) 96–100, http://dx.doi.org/10.1016/j.physe.2008.06.018.
[20] Q.J. Feng, S. Liu, Y. Liu, H.F. Zhao, J.Y. Lu, K. Tang, et al., Influence of Sb doping on the structural, optical and electrical properties of p-ZnO thin films prepared on n-GaN/Al 2 O 3 substrates by a simple CVD method, Mater. Sci. Semicond. Process. 29 (2014) 188–192, http://dx.doi.org/10.1016/j.mssp.2014.02.031.
[21] A. Phuruangrat, W. Kongpet, O. Yayapao, B. Kuntalue, S. Thongtem, T. Thongtem, Ultrasonic-assisted synthesis, characterization, and optical properties of Sb doped ZnO and their photocatalytic activities, J. Nanaomater. 2014 (2014) 10, http://dx.doi.org/10.1155/2014/725817.
[22] B.D. Cullity, S.R. Stock, Elements of X-ray Diffraction, third ed., Prentice Hall, Englewood Cliffs, NJ, 2001.
[23] A. Omidi, A. Habibi-Yangjeh, M. Pirhashemi, Application of ultrasonic irradiation method for preparation of ZnO nanostructures doped with Sb+3 ions as a highly efficient photocatalyst, Appl. Surf. Sci. 276 (2013) 468–475, http://dx.doi.org/10.1016/j.apsusc.2013.03.118.
[24] K. Ravichandran, N. Dineshbabu, T. Arun, C. Ravidhas, S. Valanarasu, Effect of fluorine (an anionic dopant) on transparent conducting properties of Sb (a cationic) doped ZnO thin films deposited using a simplified spray technique, Mater. Res. Bull. 83 (2016) 442–452, http://dx.doi.org/10.1016/j.materresbull.2016.06.033.
[25] S. Ilican, Effect of Na doping on the microstructures and optical properties of ZnO nanorods, J. Alloys Compd. 553 (2013) 225–232, http://dx.doi.org/10.1016/j.jallcom.2012.11.081.
[26] M. Caglar, F. Yakuphanoglu, Structural and optical properties of copper doped ZnO films derived by sol-gel, Appl. Surf. Sci. 258 (2012) 3039–3044, http://dx.doi.org/10.1016/j.apsusc.2011.11.033.
[27] E. Senthil Kumar, S. Venkatesh, M.S. Ramachandra Rao, Oxygen vacancy controlled tunable magnetic and electrical transport properties of (Li, Ni)-codoped ZnO thin films, Appl. Phys. Lett. 96 (2010) 1–4, http://dx.doi.org/10.1063/1.3449122.
[28] J. Mukherjee, R. Ramanjaneyulu, M.S.R. Rao, Variable range hopping crossover and magnetotransport in PLD grown Sb doped ZnO thin film, Semicond. Sci. Technol. 32 (2017) 045008, http://dx.doi.org/10.1088/1361-6641/aa5fcc.
[29] H. Liang, Y. Chen, X. Xia, Q. Feng, Y. Liu, R. Shen, et al., Influence of Sb valency on the conductivity type of Sb-doped ZnO, Thin Solid Films 589 (2015) 199–202, http://dx.doi.org/10.1016/j.tsf.2015.05.004.
[30] D.W. Zeng, C.S. Xie, B.L. Zhu, W.L. Song, A.H. Wang, Synthesis and characteristics of Sb-doped ZnO nanoparticles, Mater. Sci. Eng. B: Solid-State Mater. Adv. Technol. 104 (2003) 68–72, http://dx.doi.org/10.1016/S0921-5107(03)00314-3.
[31] S.M. Sze, Physics of Semiconductor Devices, Wiley, 1981.
[32] H.L. Mosbacker, S. El Hage, M. Gonzalez, S.a. Ringel, M. Hetzer, D.C. Look, et al., Role of subsurface defects in metal-ZnO(0001) Schottky barrier formation, J. Vac. Sci. Technol. B Microelectron. Nanometer Struct. 25 (2007) 1405, http://dx.doi.org/10.1116/1.2756543.
[33] S. Ilican, M. Caglar, S. Aksoy, Y. Caglar, XPS studies of electrodeposited grown f-doped ZnO rods and electrical properties of p-Si/n-FZN heterojunctions, J. Nanomater. 2016 (2016), http://dx.doi.org/10.1155/2016/6729032.